ResearchOnline@JCU

JAMES COOK UNIVERSITY
AUSTRALIA

THIS IS THE ACCEPTED VERSION OF THIS PAPER

Determining the Boundaries, Structure and Volume of Buried Shell Matrix Deposits using Ground-Penetrating Radar: A Case Study from Northern Australia

Selene L. Kenady[1]*, Kelsey M. Lowe[2] and Sean Ulm[1,3]

1 College of Arts, Society and Education, James Cook University, PO Box 6811, Cairns, QLD 4870, Australia

2 Institute of Resilient Regions, School of Arts and Communication, The University of Southern Queensland, Toowoomba, QLD 4350, Australia

3 ARC Centre of Excellence for Australian Biodiversity and Heritage, James Cook University, PO Box 6811, Cairns, QLD 4870 Australia

* Corresponding author

Abstract

Ground-penetrating radar (GPR) is used in this study to delineate the extent and internal structure of a large late Holocene buried shell matrix site at Thundiy, Bentinck Island, northern Australia. Shell matrix sites comprise a key component of the coastal archaeological record. The extensive nature of many shell matrix sites presents challenges for archaeological sampling regimes. While large-scale excavation is undesirable and impractical, limited test pits often represent only a tiny fraction of large shell deposits and are rarely considered representative. This study transforms GPR data into three-dimensional models which form the basis of deposit volume estimates. Volume estimates are evaluated against excavation data to test their accuracy. Results demonstrate that this novel methodology can generate accurate three-dimensional representations of buried shell matrices and highly accurate volume estimations with error margins of 3.5%±7%. It is recommended, though, that more inclusive error margins of 19.5%±17% are used to account for potential error, especially where results cannot be verified. This greater understanding of the extent and structural variability of deposits can be utilised to create robust sampling strategies for excavation. The methodology could also be further employed to enhance comparative regional studies and to add to conservation and management practices of buried shell matrix sites. If applied more widely this methodology will not only benefit our understanding of shell matrix deposits but also the wider archaeological record of coastal regions worldwide.

Keywords

geophysics; shell matrix; ground-penetrating radar; shell midden; Australian archaeology

Highlights

- GPR data were used to create volume and 3D models of buried shell matrix deposits
- Volume estimates were evaluated against excavation data
- GPR volume estimates found to be accurate within 3.5%±7%

Funding sources

1. Introduction

Shell middens are a significant component of the coastal archaeological record, but they are notoriously difficult to study. Shell matrix sites are often large and structurally heterogeneous with complex formation histories. For large stratified shell matrix sites the majority of the deposits are buried making the design of appropriate and representative sampling regimes challenging. Without total excavation the population from which the sample was taken will never be fully understood. This study addresses these challenges by employing ground-penetrating radar (GPR) to map the structure and boundaries of buried shell matrix deposits, then transforming these survey results into three-dimensional models and volume estimates of the deposits. This study establishes the specific methods for transforming GPR data into volume estimates and three-dimensional (3D) models, and tests the accuracy of these models and estimates against data generated via excavation. This methodology allows for characterisation of the size and shape of buried matrices, creating a better understanding of the population from which samples are drawn without requiring extensive excavation. The methodology also has implications for conservation efforts such as cultural heritage and community-based management plans; by creating a better understanding of buried sites without destroying the archaeological record in the process.

2. Background

There has been limited research bringing quantitative approaches to sampling issues in shell matrix research. O'Neil (1993), Poteate and Fitzpatrick (2013), and Treganza and Cook (1948) all excavated large proportions of shell matrix sites to establish the sampling size and strategy required to produce an accurate understanding of the population of the entire matrix. Bailey (1975) and Greenwood (1961) focused on how much excavated shell material was needed to be analysed in detail to characterise the overall sample accurately. The results of these studies varied significantly, illustrating just how difficult it is to create sampling regimes which appropriately characterise shell matrix sites, and how different research aims can have a significant impact on what constitutes an 'appropriate' sample. All of the studies emphasised that the samples they found necessary to accurately characterise the site being examined were not necessarily suitable for other sites. These prior approaches do not create a secure basis for addressing sampling issues in shell matrix research; this study suggests new approaches need to be established.

The most significant challenge in designing appropriate sampling regimes is in understanding the full scope of the buried matrix. Only three studies have attempted to calculate the total volume of buried shell matrix deposits (Shenkel 1986; Sorant and Shenkel 1984;Treganza and Cook 1948), but these studies failed to determine the extent of the buried deposits without full excavation. Total excavation of shell matrix sites is undesirable both in terms of expenditure and destruction of the archaeological record. However, the issue of establishing buried deposit boundaries without total excavation can be addressed via the exploratory capabilities of geophysical surveys.

To date there have been few applications of geophysical surveys in shell matrix research. An extensive literature review of the application of geophysical surveys to the investigation of shell matrix sites found only 23 papers (Table 1) representing 18 case studies (three of the case studies were represented in multiple published papers). These 23 articles included three geological studies (Dougherty and Dickson 2012; Neal et al. 2002; Weill et al. 2012) and 16 archaeological case studies. The geophysical methods employed included GPR, magnetometry, electrical resistivity, magnetic susceptibility, seismic refraction, electromagnetic induction (EM) and terrestrial laser scanning (TLS). While multiple studies addressed locating buried shell

deposits, features within the deposits and site formation, none used the geophysical methods to create three-dimensional models of the deposits and only the Larsen et al. (2017) study quantified the deposits. However, to quantify the deposits Larsen et al. utilised TLS (also called terrestrial LiDAR) which is limited, in that it cannot differentiate between shell matrices and surrounding deposits nor can it characterise buried deposits; only the mounded matrix above the surrounding ground plane.

Beyond shell matrix research, there have been efforts to create volume estimates for buried matrices from geophysical survey results. However, only one of these can be tied to archaeological research (Kristiansen 2013). The current study found the processing steps detailed by Kristiansen (2013) to be an invaluable insight into how to transform geophysical data into volume estimates and 3D models in ArcGIS. Kristiansen's methods were used as the basis for the methods employed in this study (detailed in Section 3.5) which were then altered and expanded where required.

Aside from the paper by Larsen et al. (2017) employing TLS these volume estimate studies have all employed GPR and electrical resistivity (Table 2). Of the papers reviewed, only four studies verified the results via independent methods while only seven provided error margins on their estimations (with two of the papers doing both). Navarro et al. (2014) present one of the most thorough error estimations, from which they concluded that the error margin on the volume estimates for the glaciers studied amounted to 4–8% of the total volume. Baojuan et al. (2015) and Wang et al. (2014) examined at system error and determined low ranges (1.18% and 1.2–5% respectively). Ai et al. (2014) and Binder et al. (2009) both reported significant errors (20–50%) in their kriging interpolation (a common statistical technique for modelling interpolated values) due to sparse data sets and errors in spatially locating the survey results.

3. Materials and Methods

3.1 Geophysical Survey

The survey was conducted at the large archaeological shell matrix complex of Thundiy on the northern end of Bentinck Island in the southern Gulf of Carpentaria, Queensland, Australia (Figure 1). Ground reconnaissance survey and previous excavations determined that the cultural deposits present at Thundiy extend for approximately 4km along a beach ridge to a depth of approximately 40cm. The main surface deposits are on the crest and seaward side of the beach ridge (Moss et al. in press; Nagel et al. 2016; Peck 2016). Surface scatters of shell material, however, are visible extending from the high tide mark up to 150m inland. With 4km of deposits reaching up to 150m inland and to depths of 40cm the overall shell matrix could potentially comprise up to 240,000m³ of shell material.

A MALÅ GeoScience GPR was employed, utilising a 500MHz shielded antenna with the Ramac XV monitor and the X3M control box. During the survey, the GPR system was standardly set with the number of samples at 1016 and the trace stacking set to four. The antenna and the settings employed were chosen based on knowledge of the survey site gained through prior excavation.

Table 1. Summary of geophysical studies investigating shell matrix sites, by geophysical technique.

Publication	Magnetometry	Magnetic Susc.	EM	GPR	Electrical Res.	Other
Arias *et al.* (2017)	x					
Arnold *et al.* (1997)	x			x		
Bērziņš *et al.* (2014)	x			x		
Chadwick and Madsen (2000)				x		
Connah *et al.* (1976)	x	x				
Dalan *et al.* (1992)	x				x	x (Seismic Refraction)
Dougherty and Dickson (2012)				x		
Larsen *et al.* (2017)						x (TLS)
Lowe (2010)					x	
Moffat *et al.* (2008)	x		x			
Neal *et al.* (2002)				x		
Pluckhahn *et al.* (2009)				x	x	
Pluckhahn *et al.* (2010)				x	x	
Pluckhahn *et al.* (2016)				x		
Rodrigues *et al.* (2009)			x	x		
Rodrigues *et al.* (2015)				x		
Rosendahl *et al.* (2014)		x				
Santos *et al.* (2009)			x			
Thompson (2007)					x	
Thompson and Andrus (2011)					x	
Thompson and Pluckhahn (2010)				x	x	
Thompson *et al.* (2004)	x		x	x	x	
Weill *et al.* (2012)				x		

Table 2. Breakdown by geophysical technique of papers utilising geophysical surveys to create volume estimates.

Publication	Geological Medium	GPR	Electrical Res.	TLS
Ai *et al.* (2014)	Glacier ice	x		
Baojuan *et al.* (2015)	Glacier ice	x		
Binder *et al.* (2009)	Glacier ice	x		
Colucci *et al.* (2015)	Glacier ice	x		
Dickson *et al.* (2009)	Beach sand	x		
Kristiansen (2013)	Perennial snow patch	x		
Larsen *et al.* (2017)	Shell matrix			x
Navarro *et al.* 2014	Glacier ice	x		
Nowroozi *et al.* (1997)	Gravel deposits		x	
Prinz *et al.* (2011)	Glacier ice	x		
Rucker *et al.* (2011)	Dredgable river sediments		x	
Sambuelli and Bava (2012)	Lake water	x		
Tetegan *et al.* (2012)	Rock fragments		x	
Van Heteren *et al.* (1996)	Beach sand	x		
Wang *et al.* (2014)	Glacier ice	x		
Yde *et al.* (2014)	Glacier ice	x		

Three geophysical transects were established using a Real Time Kinematic (RTK) surveying system (Figure 1). Two adjacent transects (Transect A and B) were laid out along the ridgeline for 120m while Transect C crossed Transects A and B at right-angles, running inland for 160m. Each transect was laid out in 5m² squares: each transect measured one square (5m) wide, while Transects A and B were 24 squares long and Transect C was 32 squares long. This transect design allowed for strict grid control and for the survey to incorporate the inland and seaward boundaries of the site, while also covering the locations of the prior excavations; which ran parallel to the sea along the beach ridge. These choices were made under the constrictions of limited field time at a very remote site so the full length of the shell deposit along the ridgeline, approximately 4km based on surface scatters of shell, was not established via geophysical survey.

Survey lines were run the full length of Transects A-B and for 155m of the 160m Transect C; the survey started 5m in from the seaward end of the transect to avoid pandanus palms. String lines were run every 1m to 1.5m as survey guides along the transects. Survey lines were run every 50cm. Prior to survey, the site was hand cleared using secateurs and cane knives to remove as much of the vegetation (mostly grass clumps) as possible. The remaining stubble was low enough to create a relatively smooth surface for the GPR to run over, this was done to reduce coupling loss and coupling changes.

3.2 Excavation

Previous excavations provided information concerning the chronostratigraphy of the midden deposit at Thundiy. Excavation squares (Squares A, B and C) had been placed along the ridge line down what was considered to be the main body of the shell deposit based on a visual site inspection of the surface (Figure 1). The geophysical grid was placed over these squares to take advantage of the stratigraphic information they provided. Further excavation was also undertaken at the edges of the shell matrix deposits with two more squares (Squares D and E) placed within geophysical Transect C beyond the main body of the deposit, but in locations where shell material was still visible on the surface (Figure 1).

The three original excavations (Squares A-C) revealed remarkably similar deposits along the ridge (Figure 2). The squares were excavated to approximately 60cm, and each consisted of a layer of dense cultural shell at the surface overlaying natural beach ridge deposits with a basal layer of consolidated beachrock material (Nagel et al. 2016). Stratigraphic Unit I (SUI) represents the dense cultural shell matrix present at the surface exhibiting well-preserved cultural shell material including charcoal fragments, stone artefacts and bone fragments in a dark brown humic sediment. This layer extends from the surface to 15cm for Square A, 35cm for Square B and 27cm for Square C (Nagel et al. 2016). SUIIa and SUIIb represent a transitional zone exhibiting a mixing of cultural shell material with underlying natural shell deposit material. SUIIa is characterised by a continuation of the dark brown humic sediment present in the cultural matrix but with decreasing shell material; this layer ranges in thickness from 15cm in Square A, and 5cm in Square B to 8cm in Square C. SUIIb exhibits a less humic sediment considered to be non-cultural in origin, containing numerous pisoliths and small (<10mm) gastropods indicative of natural beach ridge deposits. SUIII represents sandy beach ridge material composed of shell grit with pebble and coral inclusions in a medium-grained siliciclastic sand (Nagel et al. 2016). Chunks of consolidated beachrock were found towards the base of the excavations.
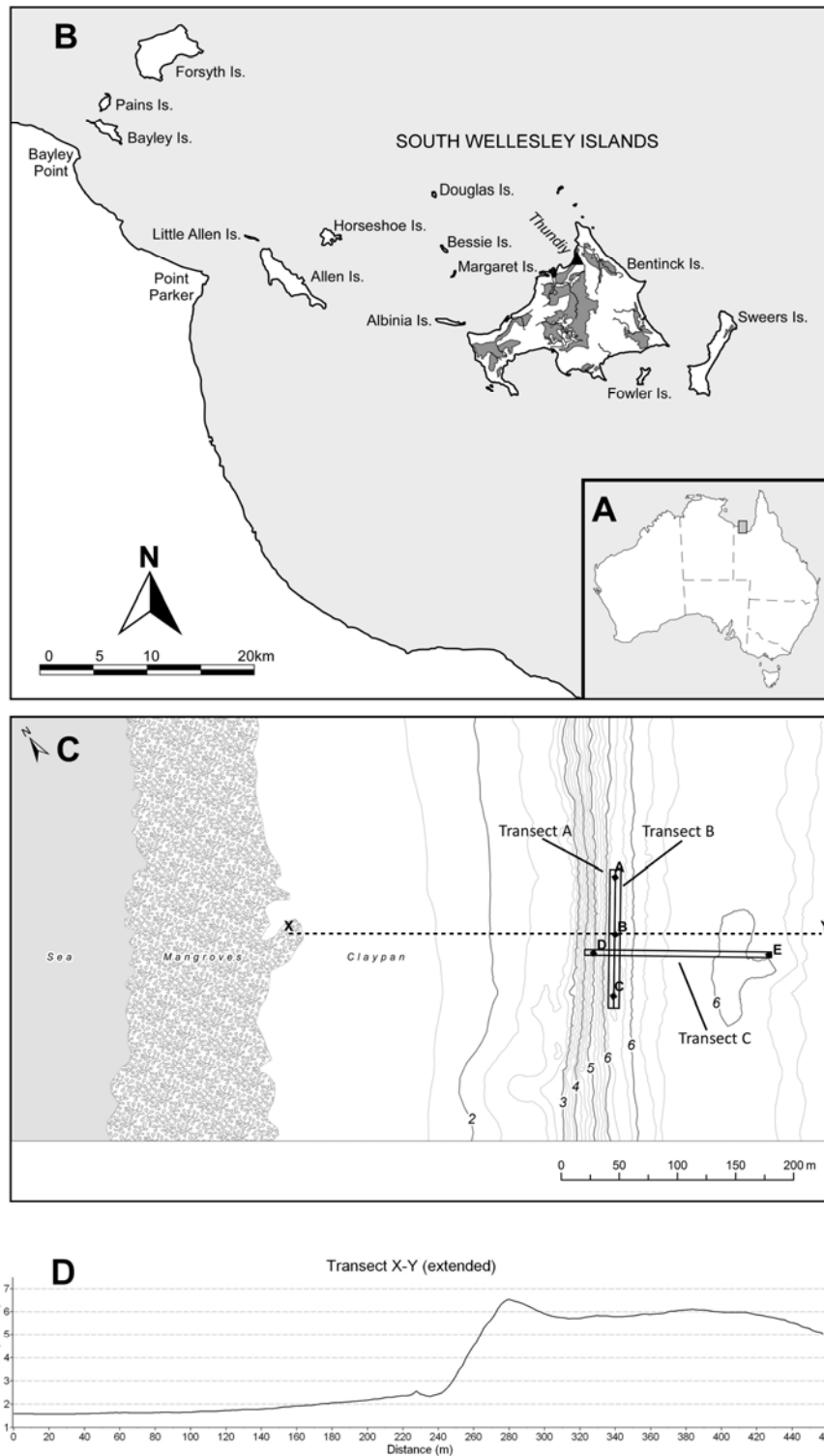
Figure 1. (A–B) The South Wellesley Islands, southern Gulf of Carpentaria, Australia, showing the location of Thundiy on the north coast of Bentinck Island. (C) Topographic map of the central area of Thundiy indicating the location of excavation squares A–E (solid squares) and GPR Transects A-C (open rectangles). (D) Cross-section X–Y (as shown in C). Elevations are relative to Australian Height Datum (AHD).
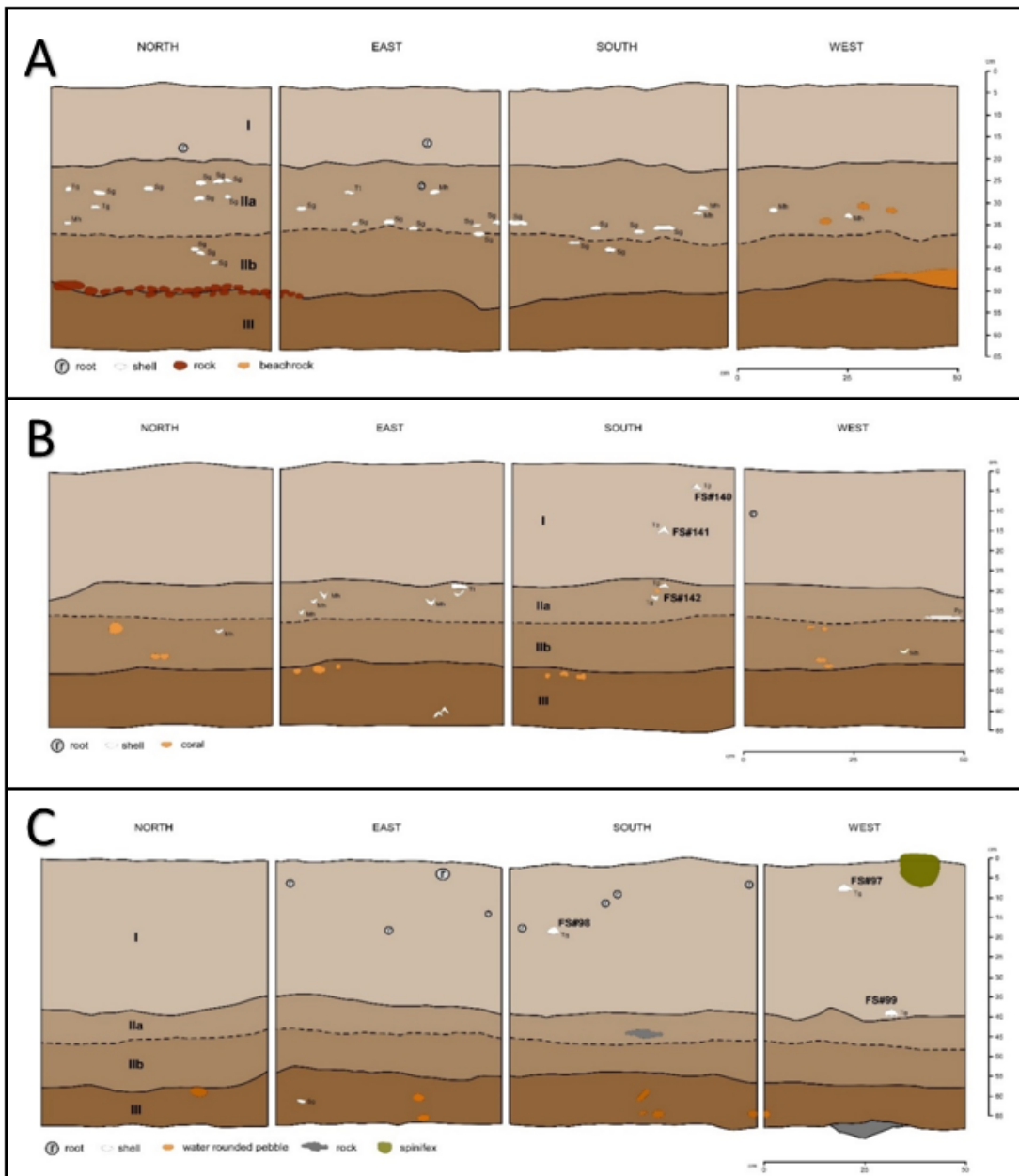
Figure 2. Thundiy sections diagrams for (A) Square A, (B) Square B and (C) Square C.

The excavated squares situated at the edges of the midden, Squares D and E, were considerably different to Squares A, B and C. Square D revealed a mix of cultural midden and natural beach ridge material (SUI) over a pisolith and small gastropod-rich beach ridge deposit (SUII and SUIII) terminating in a bowl-shaped structure in the beachrock (Figure 3). The bowl-like feature in the rock began at 33.6cm below the ground surface and continued to a depth of 55.8cm.
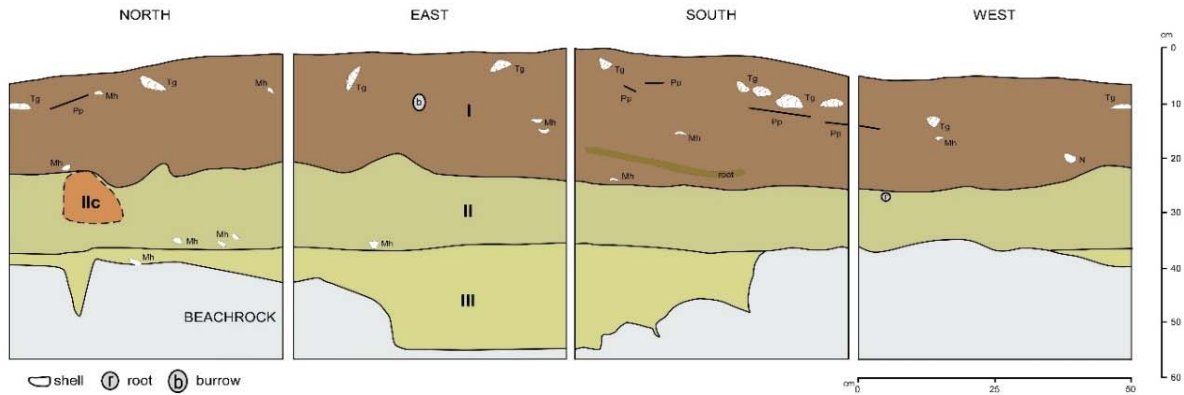

Figure 3. Thundiy sections diagram for Square D.

Square E was placed well beyond the edge of the main midden deposits, but in an area where small amounts of shell material were still visible in low densities on the surface. Square E,a 1m by 1m shovel test pit, confirmed that the shell material present on the surface was not related to buried midden deposits (Figure 4). The excavation revealed very sparse cultural shell in a humic layer at the surface (SUI) to about 25cm, below which was iron-rich red sands (SUII to SUV) with increasing pisolith numbers from 60cm the base of the square at 115cm (SUIII, SUIV and SUV).
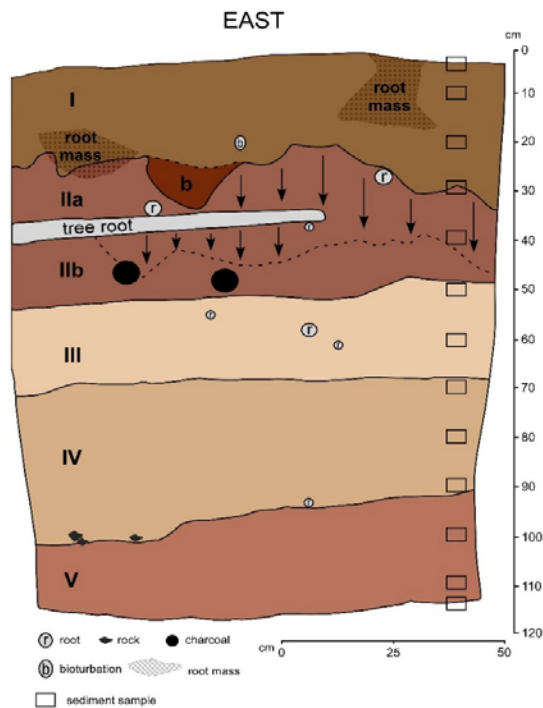

Figure 4. Thundiy sections diagram for Square E.

3.3 AMS Radiocarbon Age Determinations

Radiocarbon dating showed consistent chronostratigraphic relationships between excavations for Squares A to C (see Nagel et al. 2016 for full details of radiocarbon determinations). Surface deposits (SUI) dated to around 130 cal BP, with dates below ranging back to 700–800 cal BP for the lower cultural deposits (SUI and SUIIa). Below 40cm (SUIIb) there is a sharp stratigraphic disjunction where the cultural deposits end and the dates for the underlying natural deposits jump to 4000–5000 cal BP. Based on these dates, the cultural shell deposits for Thundiy represent a recent initiation of cultural occupation on a much older land surface, with the natural beach ridge deposits having been formed >3,000 years prior. The shell embedded in the beachrock of Square D gave a slightly older age of approximately 5334 cal BP (see Nagel et al. 2016).

3.4 Survey Data Processing

For processing, the MALÅ files were imported into Reflexw. The files were initially *time-cut* to the top 100ns to remove extraneous depth. Further data processing proceeded in this order: *subtract mean* (also called *dewow*), *static correction*, *manual gain* (*y*), *background removal*, a *bandpass filter* (*butterworth*). Then a *Kirchhoff 2D-velocity migration* and a *time-depth conversion* were completed based on a *hyperbola* (or *velocity*) adaption. As the final processing step, the reflection profiles were topographically corrected. With the files fully processed the *pick* function in Reflexw was used to mark planar reflections in the profiles that correlated with the shell matrix deposit boundaries as established through excavation. A summary of the data processing workflow appears in Figure 5.
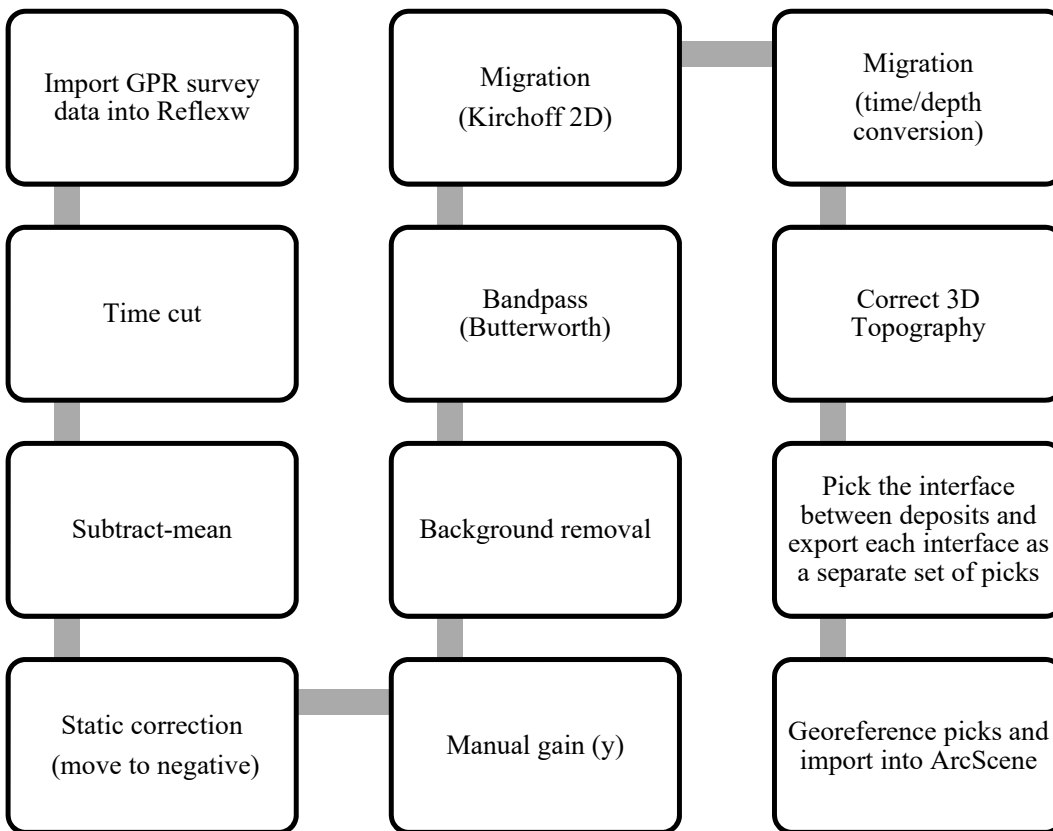

Figure 5. Data processing workflow for GPR survey data.

The GPR results for Transects A and B show four distinctive planar reflections of high amplitude between the top of the profile down to 80cm which is c.60cm from the ground surface (Figure 6, see also Supplementary Data for full profiles and for the full dataset see: http://dx.doi.org/10.4225/28/584755108d3dc). These reflections match the cultural shell deposits observed in stratigraphic units SUI and SUIIa of Squares A to C (Figure 7). The planar reflections at the surface are interpreted as representing the cultural shell matrix present on site, and the base reflection in this series of reflections was 'picked' (Supplementary Data). In Transects A and B a separate high amplitude planar reflection off a subsurface linear interface is visible in the profile at approximately 110cm depth (or 90cm below the ground surface). This second planar reflection is located in the region of the basal beachrock present below sedimentary unit SUIII and was interpreted as representing this feature. This reflection was 'picked' as a separate layer, and both layers were exported to Microsoft Excel where 'picks' were assigned georeferenced coordinates based on information generated from ArcMap before being exported to ArcGIS for the creation of volume estimates and 3D models.
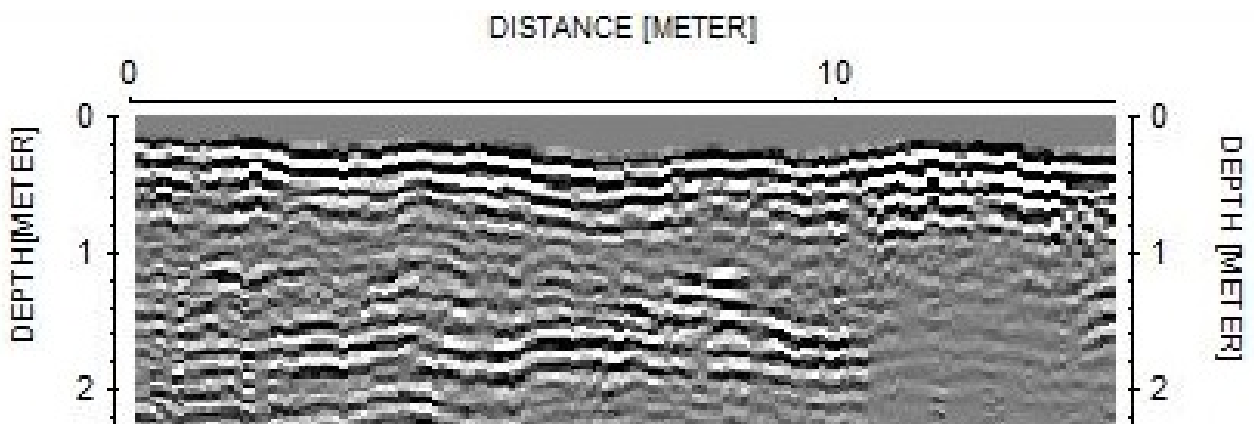

Figure 6. Detailed view of Thundiy GPR Line 3 of Transect A-B, from 0m–12m.
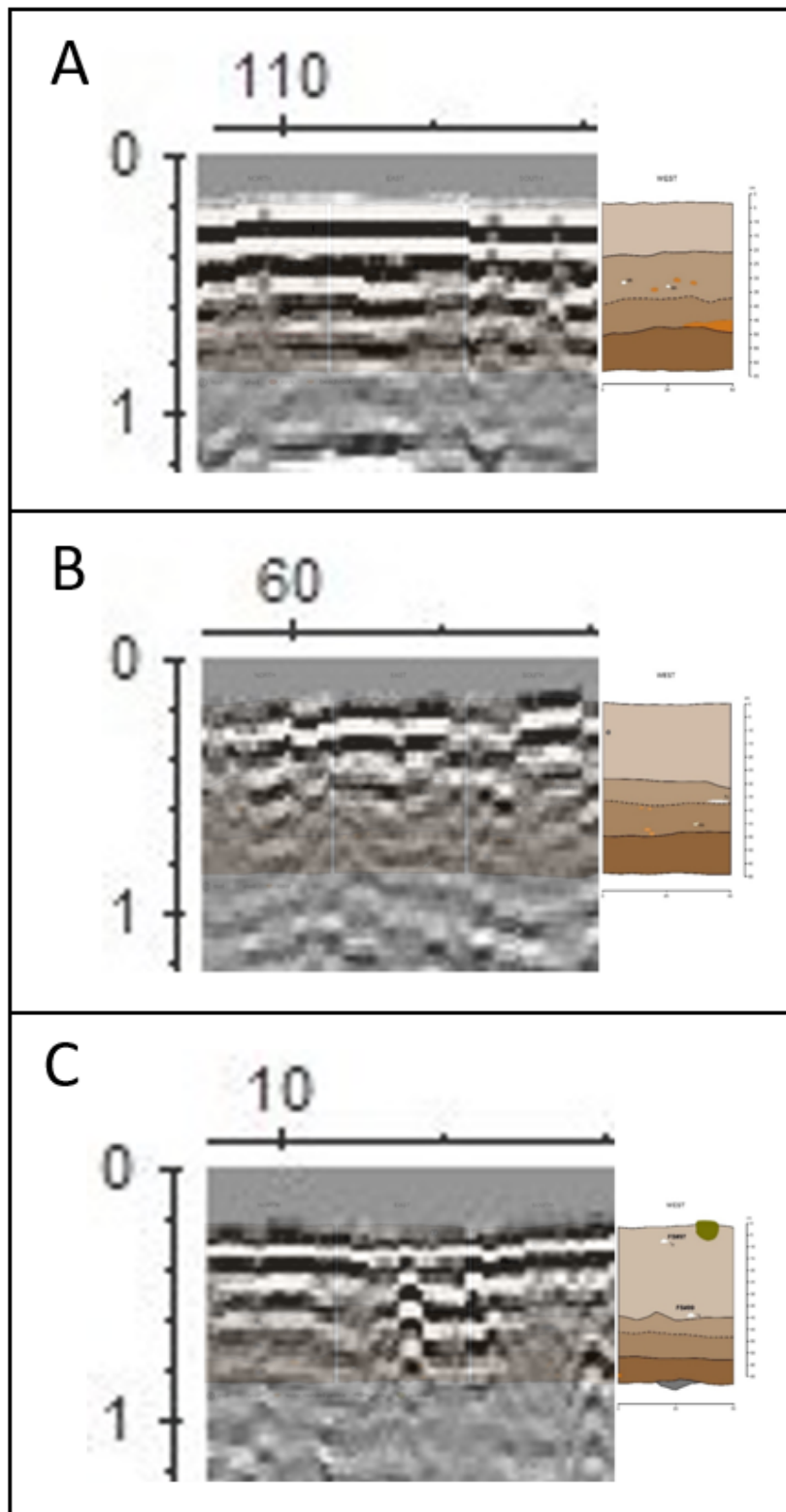
Figure 7. Comparison of stratigraphic units with GPR reflection profiles from the same location; horizontal scale has been greatly exaggerated for the sections diagrams so that an accurate vertical scale could be achieved. (A) Square A, (B) Square B and (C) Square C.

The results for Transect C were less distinctive (Figure 8). There was no clear difference in Transect C between the cultural deposits and the beachrock, so a single deposit was 'picked'. The high amplitude planar response present in the results for Transect C extends to c.100cm in depth from the ground surface and was interpreted as including all deposits above the beachrock, consistent with the interpretations of Transects A and B. The main body of the feature appears to end at approximately 40m along the transect (Supplementary Data). The 'picks' for this deposit were exported to Microsoft Excel where they were georeferenced, then exported to ArcMap. Beyond this first 40m, intermittent areas of high amplitude response are visible, at 42–54m and particularly at 65–75m and again from 120m to the end of the profile (Supplementary Data). The high amplitude responses visible in the profiles from 42–54m and from 120–155m were interpreted to be the result of tree roots as there were several large trees mapped adjacent to Transect C in these locations. The high amplitude response from 65–75m is noteworthy, however, as there were no significant trees in this area though there was a patch of dense shell material at the surface. This anomaly also exhibits a sloping planar interface dipping away from the high amplitude response at the surface. This sloping interface may be a potential palaeosurface, though excavation would be required to confirm this interpretation.
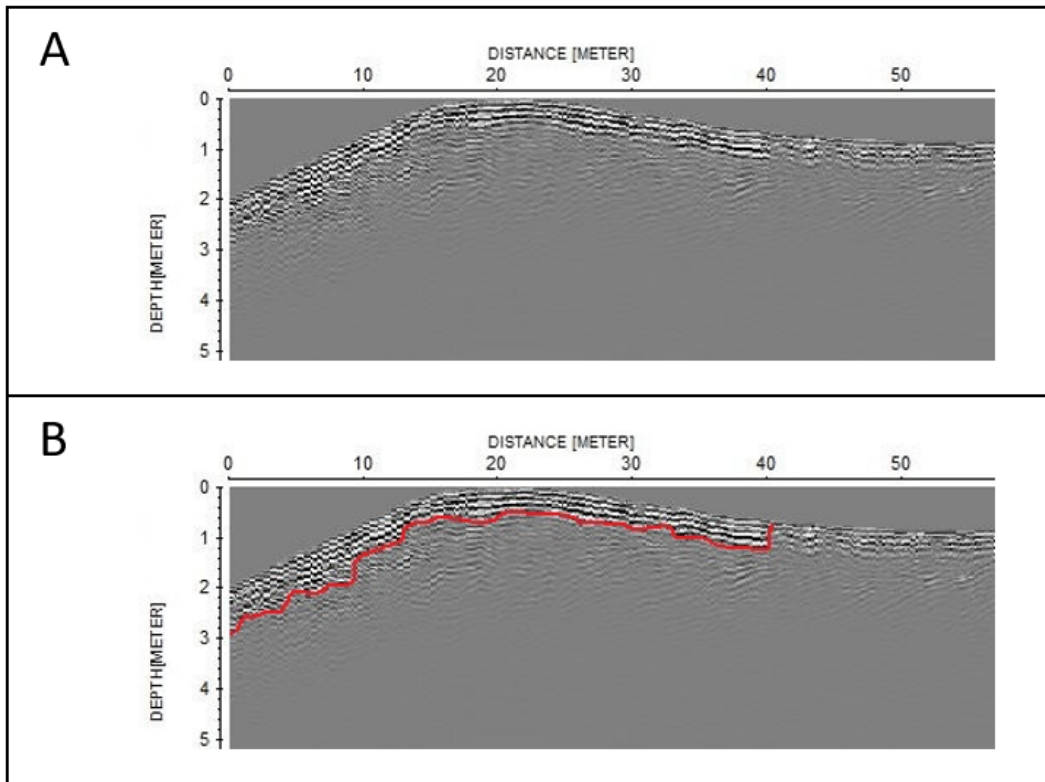

Figure 8. Thundiy GPR Line 1 of Transect C. (A) Un-interpreted profile and (B) Interpreted profile. The red line marks the high amplitude planar anomaly representing the shell matrix and beachrock combined which ends at around 40m along the profile.

3.5 Three Dimensional Data Processing

This study found that the range of processing software available for GPR data allows for the creation of 3D volumes for the full survey results but not for the isolation of individual deposits. In order to create volume estimates and 3D models of individual deposits, within the GPR data, another processing software had to be sourced. The literature review conducted for this study discovered only one reference for creating 3D models and volume estimates from GPR data; which was Kristiansen's (2013) Master's thesis. Kristiansen employed the ArcGIS software suite (ArcScene and ArcMap) to model the results. This study adopted the basic procedure from Kristiansen and then relied on Esri help forums to trouble shoot and fill in any gaps in the methods.

Calculating a volume estimation for the deposit required both ArcMap 10.2.1 and ArcScene 10.2.1 to complete different functions required for mapping the deposits (Figure 9). As the RTK was not connected to the GPR during the survey, survey lines were manually georeferenced to locate them accurately within the survey grids in ArcGIS. Thundiy had been mapped extensively with an RTK. The RTK points were imported into ArcScene and used to create a triangulated irregular network (TIN) of the surface topography of the site. A second and third TIN (where more than one boundary was being represented) were created based on the deposit boundaries as delineated in the geophysical survey results. The TINs were then used to create volume calculations and 3D polygon models of the buried deposits. Unfortunately, these 3D images cannot be exported from ArcScene with a scale bar, north arrow or key as ArcScene (unlike ArcMap) has no *layout view*.
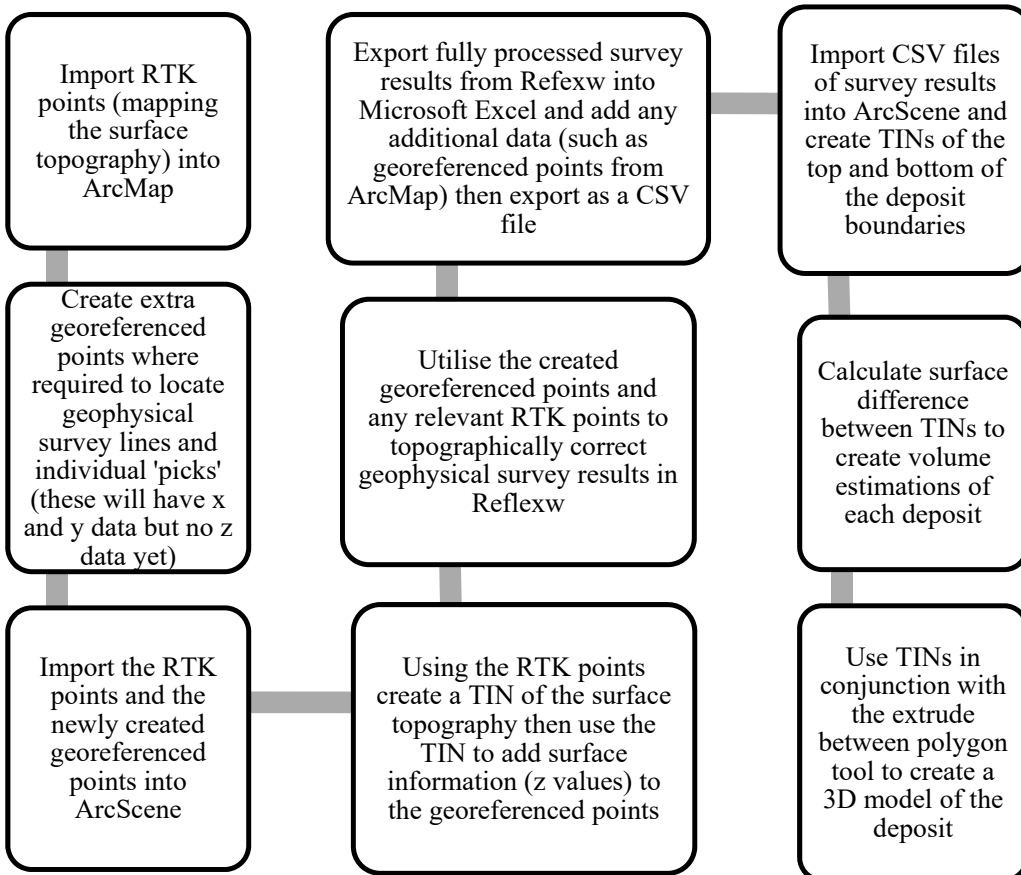
Import RTK points (mapping the surface topography) into ArcMap	Export fully processed survey results from Refexw into Microsoft Excel and add any additional data (such as georeferenced points from ArcMap) then export as a CSV file	Import CSV files of survey results into ArcScene and create TINs of the top and bottom of the deposit boundaries
Create extra georeferenced points where required to locate geophysical survey lines and individual 'picks' (these will have x and y data but no z data yet)	Utilise the created georeferenced points and any relevant RTK points to topographically correct geophysical survey results in Reflexw	Calculate surface difference between TINs to create volume estimations of each deposit
Import the RTK points and the newly created georeferenced points into ArcScene	Using the RTK points create a TIN of the surface topography then use the TIN to add surface information (z values) to the georeferenced points	Use TINs in conjunction with the extrude between polygon tool to create a 3D model of the deposit

Figure 9. Data processing workflow for ArcGIS and ArcScene.

To check the volume estimates created from the survey results against the real site conditions, the modelled estimates for Squares A to C were compared to estimates produced from the excavated material. The cultural shell volume for the excavated material was calculated for each excavation square as the volume of a cube (50cm x 50cm x depth of shell deposit), with the deposit depth based on observations of the shell content. This estimation is an approximation as the base of the deposits were not perfectly square. The majority of cultural shell material was recovered in the top 36cm for Square A, 37cm for Square B and 30cm for Square C (Peck 2016:125). The total shell matrix (cultural and natural) for the excavation squares could only be calculated to the base of the excavations, which ended at 61cm for Square A, 60.8cm for Square B, and 60cm for Square C. For Square D, the curved basin in the beachrock meant the excavated volume had to be calculated by adding the volume for the top of the excavation (a rectangular prism) to the volume for the bottom of the excavation which most closely matched half a sphere. The excavated volume for Square D can be expected to be close to the actual volume, but not exact, as the basin was not an exact hemisphere.

The two volume estimations (based on the excavated material and the GPR survey results) were then compared by calculating the difference between the two and creating a percentage error based on this difference (Equation 1).

% error = ([actual value - experimental value] / actual value) x 100   (Equation 1)

Initial results for the cultural shell in Squares A-C showed a significant difference between the two estimates that indicated it was possible an error had occurred (Table 3). The most obvious source of error was that the 'picks' might have been inaccurately placed on the profiles. This possibility was reviewed and it was observed the 'picks' had initially been placed on the fourth and final planar reflection at the top of the profile which actually places the picks closer to the top of SUIII (the culturally sterile matrix) instead of at the base of SUIIa (see Figure 7). This fourth reflection, though it coincides with the top of SUIII is unlikely to be a reflection from that deposit as the gradient between it and SUIIb is gradual and unlikely to be significant enough to create a genuine reflection. It is more likely that this reflection is a multiple of the reflections above. Multiple reflections (or multiples) occur when the radar wave reflects back and forth between the surface and a subsurface layer (Conyers 2004:126). The volume estimate generated from the GPR survey compared to the excavation results indicated the 'picks' were off by an average of 15cm which, due to the scale of the profile, was the difference between the final planar reflection and the reflection directly above it (Figure 10). This was visually a small mistake to make, yet it had a significant impact on the results. The second round of 'picks' were created based on this information. These results were then processed in ArcScene, with volume estimates and 3D models generated. The results (presented in Section 4) showed a vast improvement in the relationships between the volume estimates made from the GPR results and those from the excavation.

Table 3. Initial Cultural shell matrix volume Thundiy, Squares A-D.

Thundiy Excavation	Cultural Shell Matrix Volume (m³) Based on GPR Survey Results	Cultural Shell Matrix Volume (m³) Based on Excavation	Modelling Compared to Excavated Volume (m³)	Error Percentage
Square A	0.12	0.09	+0.03	33% (Overestimate)
Square B	0.13	0.09	+0.04	44% (Overestimate)
Square C	0.11	0.07	+0.04	44% (Overestimate)
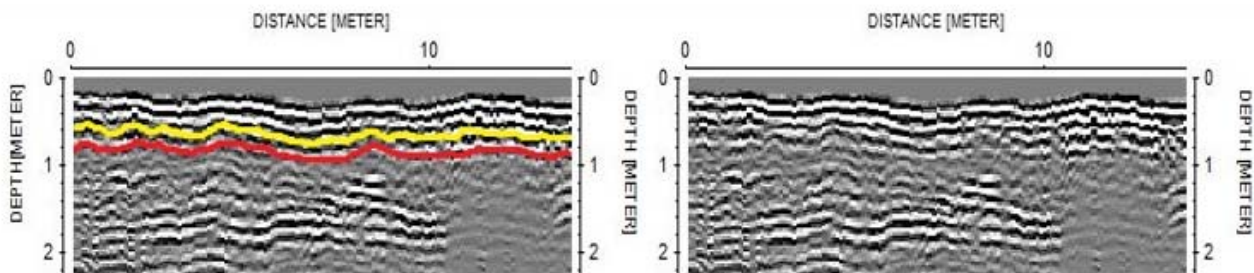
Figure 10. Extract of Line 4 (Transects A-B) at Thundiy showing the placement of the 'picks' marked in red and the placement of the actual shell deposit marked in yellow (left). An unedited extract of Line 4 is provided for visual comparison (right).

4. Results

By mapping the GPR survey results for Thundiy into ArcScene (via processing in ArcMap) a 3D model of the shell matrix deposits for Transects A, B and C was created (Figure 11). The cultural and natural deposits were separated for Transects A and B but this was not possible for Transect C, and so the deposits were mapped together. Volume estimates were also created in ArcScene, and the total shell matrix volume for Transect C was calculated to be 108.27m³ while the total for Transects A and B was 1,105m³ with the cultural shell making up 385.92m³ of this larger deposit. Based on the results for Transect C this would bring the total volume estimation for the combined cultural and natural shell deposits at Thundiy down to around 86,616m³ instead of the 240,000m³ initially estimated; as the buried matrix was found to end around 40m inland rather than extending the full 150m in which shell material can be seen on the surface. Based on the results from Transects A and B, the cultural shell volume estimation for the entire site at Thundiy would be c.51,455m³.
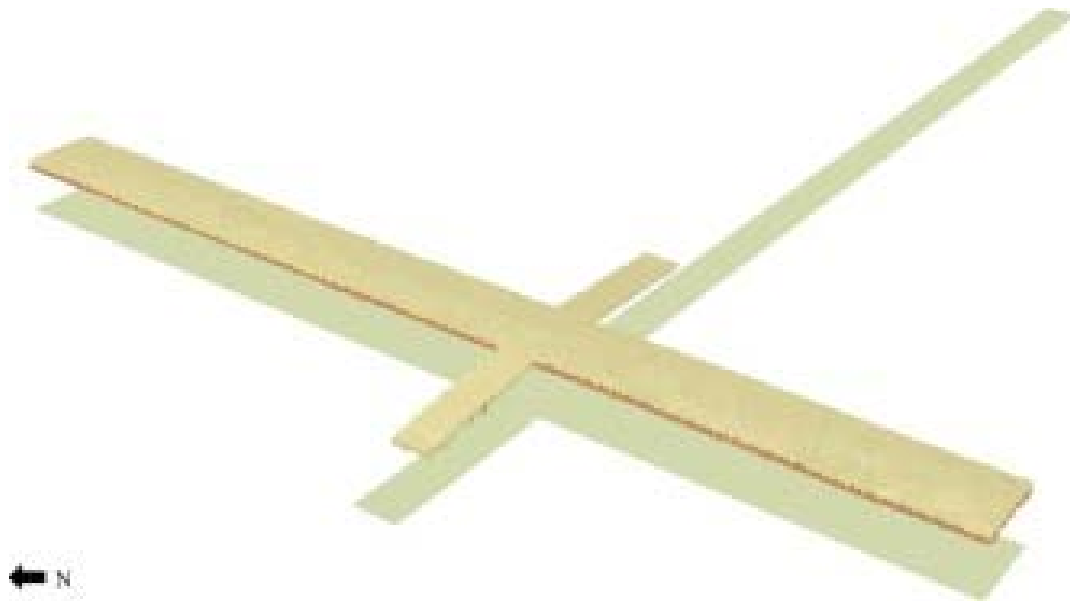
Figure 11. Thundiy shell matrix deposits for Transects A-B (120m by 10m) and C (40m by 5m) as viewed from the south-west. Transects A-B exhibit both the upper cultural deposits (tan upper layer) and the lower total shell deposit including both cultural and natural shell material (brown lower layer). The green cross underneath represents the full Transects A-B (120m by 10m) and C (160m by 5m).

The cultural shell volume estimates matched the excavation estimates from Squares B and C, while underestimating the deposits of Square A by 11% (see Table 4). The total shell matrix volume (cultural and natural shell material) based on the GPR survey significantly overestimated the deposits for Squares A, B and C compared to the results calculated from the excavations (Table 5). Though this is to be expected, as the excavations for Squares A-C reached fine sandy sediments but did not fully expose the beachrock thought to underlay the shell matrix, which makes these excavated estimates an underestimate of the actual volume by an unknown margin. In contrast, the beachrock was fully exposed for Square D and here the volume calculations match well, with a modelled volume of 0.22m³ compared with 0.23m³ for the excavated results. The results for Square D thus indicate that the volume estimations calculated from the GPR survey results may be closer to the actual in-ground matrix than the excavated volume estimations from Squares A-C indicate.

Table 4. Cultural shell matrix volume Thundiy, Squares A-D.

Thundiy Excavation	Cultural Shell Matrix Volume (m³) Based on GPR Survey Results	Cultural Shell Matrix Volume (m³) Based on Excavation	Modelling Compared to Excavated Volume (m³)	Error Percentage
Square A	0.08	0.09	-0.01	11% (Underestimate)
Square B	0.09	0.09	0.0	0%
Square C	0.07	0.07	0.0	0%

Table 5. Total shell matrix volume Thundiy, Squares A-D.

Thundiy Excavation	Total Shell Matrix Volume (m³) Based on GPR Survey Results	Total Shell Matrix Volume (m³) Based on Excavation	Modelling Compared to Excavated Volume (m³)	Error Percentage
Square A	0.22	0.15	+0.07	46% (Overestimate)
Square B	0.24	0.15	+0.09	60% (Overestimate)
Square C	0.23	0.15	+0.08	53% (Overestimate)
Square D	0.22	0.23	-0.01	4% (Underestimate)

Confidence intervals were calculated for the mean error percentages exhibited for the volume estimates (all confidence intervals presented have been rounded to the nearest 0.5%). These confidence intervals were produced using Equation 2 and were calculated for a 95% confidence level.

$$\bar{X} \pm t \frac{s}{\sqrt{n}} \qquad \text{(Equation 2)}$$

The confidence intervals on the error margins produced by the Thundiy results are 3.5%±7% (a range of -3.5% to 10.5%) or 19.5%±17% (2.5% to 36.5%) if the original misplaced 'pick' results for the cultural shell of Squares A-C are included. The error percentages for the total shell matrix for Squares A to C were excluded from these calculations as they were not accurately verified by excavation (with the excavation ending before fully exposing the beachrock). The upper range of the error margin (10.5%) was applied to the volume results to produce a volume range more likely to include the true shell matrix volume. For this case study, that meant that the true volume results for the total Transect C deposit should fall within a range of 108m³±11.5m³ while the cultural shell for Transects A and B should be within 386m³±40.5m³, and the total shell deposit within 1,105m³±116m³. So the overall cultural shell for the larger site at Thundiy should fall within 51,455m³±5,403m³. However, the original misplaced 'picks' show how the error values of the volume results can increase greatly. Where the volume results have not been verified via excavation, it would be more conservative to apply a confidence interval based on an error of 36.5%.

5. Discussion

GPR accurately characterised the buried shell deposits at Thundiy and provided the basis for 3D models closely matching the in-ground deposits. The volume estimates for Square D and the cultural shell matrix of Squares A-C were highly accurate once the initial misplacement of 'picks' had been corrected. The full (cultural and non-cultural) shell matrix for Squares A-C overestimated the shell deposit compared to the excavated results (by an average of 53%). However, this was owing to the excavation squares not fully exposing the beachrock at the base so an overestimation was expected and the accuracy of these results cannot be fully evaluated.

Prior research focusing on creating volume estimates from geophysical surveys accounted for estimates of system and data acquisition error. System error has been reported as relatively low, with error estimates lower than 10% (Baojuan et al. 2015; Navarro et al. 2014; Wang et al. 2014), while data acquisition error can be significant, amounting to error ranges from 20–50% (Ai et al. 2014; Binder et al. 2009;). This case study found that when correctly interpreted, the survey results can produce accurate volume estimates with an error range of only ±10.5% – higher than, but close to the error estimates of system error calculated by prior studies. Interpretation error was found to be the major source of error in this study. If the results were not archaeologically tested this error might have gone undetected, therefore it would be advisable where the results have not been verified via excavation to employ an error range of ±36.5%; a similar error value to those created by prior research experiencing data acquisition errors.

The results of this study highlight the importance of excavation verification and detailed stratigraphic analysis to the interpretation of modelled outcomes. The significant error between the modelled volume estimates produced for the cultural shell of Transects A and B and those from excavation highlighted the potential existence of an error in the modelled results. The detection of this error meant that the 'picks' could then be re-evaluated and the source of the error identified. This particular error was in the interpretation of the data, but with extensive and complex datasets it could have been an error incorporated during data conversion or collection. Detection of the error meant the results could then be reinterpreted, in this case re-picked, and the volume estimates and 3D models corrected.

Due to the nature of the methods employed in this research, with points interpolated via TIN models and with deposit boundaries 'picked' by visual interpretation, which is open to variation, the resulting 3D models and volume estimates are not a fully accurate reflection of reality. The results from this case study show how volume estimates can quickly become inaccurate by a significant margin due to misinterpretation. While inaccuracies were experienced with the volume estimates, the results produced were always broadly representative of the reality of the deposits thus providing useful information and at times even being highly accurate. The 3D models were also accurate enough to provide important information about the deposits, with the results producing interpretable models of the shape and structure of the buried matrix.

6. Conclusions

This case study showed that it is possible to create volume estimates and 3D models of buried shell matrix deposits based on geophysical survey data. Prior efforts to estimate the volume of a buried matrix from GPR data highlighted specific methods for doing so. Of particular use was Kristiansen's (2013) Master's thesis which detailed the process of creating volume estimations and 3D models of buried matrices in ArcGIS, based on GPR survey data. The methods detailed in Kristiansen's work formed the basis of the methods employed for this research.

The methodology successfully created volume estimates and 3D models of buried shell matrices. The total GPR error margin on the volume estimates, was only 16%±11%; this includes the erroneously placed 'picks' but discounts the full shell deposit results for Squares A-C (as they were not verified by excavation). Without the incorrectly placed 'picks' from Thundiy, the error margin falls to 3.5%±7%. It would be advisable, however, to apply the larger error range of 19.5%±17% as a more accurate representation of the actual error range on the GPR volume estimates. When used in conjunction with archaeological excavation this method provides a detailed understanding of the overall population from which the excavated samples were taken, thereby improving shell matrix research. These results illustrate that geophysical surveys can successfully produce information about shell matrix sites.

While this methodology was mainly developed to aid in creating appropriate sampling regimes for excavation, it could be further used to gain a greater regional understanding of shell matrix sites and to aid in conservation and management plans where applicable. Comparative regional studies would gain from a greater understanding of the size, shape and character of buried deposits which would enhance the characterisation of different site types for a region. By combining the geophysical survey results with limited excavation from which radiocarbon dates are obtained, changes in shell midden sizes and frequency, both spatially and temporally, can be investigated thereby providing insight into site formation, spatial organisation and the built environment. For conservation efforts and management plans, the more we can learn about buried deposits using non-invasive technologies, the better 'best practice' management strategies we can generate for the preservation and protection of them. Further, we can develop models and maps from this analysis to assist in site management and monitoring. Such maps and models could be used as a baseline so that if significant damage occurs to a shell matrix site, it could be re-mapped and the new data compared to the old to create a quantitative measure of the amount of shell matrix lost.

Acknowledgements

References

Ai, S., Z. Wang, E. Dongchen, K. Holmén, Z. Tan, C. Zhou and W. Sun 2014 Topography, ice thickness and ice volume of the glacier Pedersenbreen in Svalbard, using GPR and GPS. Polar Research 33(1):1-8. http://dx.doi.org/10.3402/polar.v33.18533

Arias, P., M. Diniz, M. Cubas, C. Duarte, E. Iriarte, C. Salzmann, F. Teichner and L. Teira 2017 Looking for the traces of the last hunter-gatherers: Geophysical survey in the Mesolithic shell middens of the Sado valley (southern Portugal). Quaternary International 435(B):61-70. https://doi.org/10.1016/j.quaint.2016.02.016

Arnold, J.E., E.L. Ambos and D.O. Larson 1997 Geophysical surveys of stratigraphically complex island California sites: New implications for household archaeology. Antiquity 71(271):157-168. https://doi.org/10.1017/S0003598X00084647

Bailey, G.N. 1975 The role of molluscs in coastal economies: The results of midden analysis in Australia. Journal of Archaeological Science 2(1):45-62. https://doi.org/10.1016/0305-4403(75)90045-X

Baojuan, H., L. Zhongqin, W. Feiteng, W. Wenbin, W. Puyu and L. Kaiming 2015 Glacier volume estimation from ice-thickness data, applied to the Muz Taw glacier, Sawir Mountains, China. Environmental Earth Sciences 74(3):1861-1870. https://doi.org/10.1007/s12665-015-4435-2

Bērziņš, V., U. Brinker, C. Klein, H. Lübke, J. Meadows, M. Rudzīte, U. Schmölcke, H. Stümpel and I. Zagorska 2014 New research at Riņņukalns, a Neolithic freshwater shell midden in northern Latvia. Antiquity 88(341):715-732. https://doi.org/10.1017/S0003598X0005064X

Binder, D., E. Brückl, K.H. Roch, M. Behm, W. Schöner and B. Hynek 2009 Determination of total ice volume and ice-thickness distribution of two glaciers in the Hohe Tauern region, Eastern Alps, from GPR data. Annals of Glaciology 50(51):71-79. https://doi.org/10.3189/172756409789097522

Chadwick, W.J. and J.A. Madsen 2000 The application of ground-penetrating radar to a coastal prehistoric archaeological site, Cape Henlopen, Delaware, USA. Geoarchaeology 15(8):765-781. https://doi.org/10.1002/1520-6548(200012)15:8<765::AID-GEA2>3.0.CO;2-H

Colucci, R.R., E. Forte, C. Boccali, M. Dossi, L. Lanza, M. Pipan and M. Guglielmin 2015 Evaluation of internal structure, volume and mass of glacial bodies by integrated LiDAR and ground penetrating radar surveys: The case study of Canin Eastern Glacieret (Julian Alps, Italy). Surveys in Geophysics 36(2):231-252. https://doi.org/10.1007/s10712-014-9311-1

Connah, G., P. Emmerson and J. Stanley 1976 Is there a place for the proton magnetometer in Australian field archaeology? Mankind 10(3):151-155. https://doi.org/10.1111/j.1835-9310.1976.tb01145.x

Conyers, L.B. 2004 Ground-Penetrating Radar for Archaeology. Plymouth, UK: AltaMira Press.

Dalan, R.A., J.M. Musser and J.K. Stein 1992 Geophysical exploration of the shell midden. In J.K. Stein (ed.), Deciphering a Shell Midden, pp.43-59. San Diego, CA: Academic Press Inc.

Dickson, M.E., C.S. Bristow, D.M. Hicks, H. Jol, J. Stapleton and D. Todd 2009 Beach volume on an eroding sand-gravel coast determined using ground penetrating radar. Journal of Coastal Research 25(5):1149-1159. https://doi.org/10.2112/08-1137.1

Dougherty, A.J. and M.E. Dickson 2012 Sea level and storm control on the evolution of a chenier plain, Firth of Thames, New Zealand. Marine Geology 307-310:58-72. https://doi.org/10.1016/j.margeo.2012.03.003

Greenwood, R.S. 1961 Quantitative analysis of shells from a site in Goleta, California. American Antiquity 26(3):416-420. https://doi.org/10.2307/277409

Kristiansen, J. 2013 Fra Natur Til Kart: Veien til 3D-modellering av en isfonn ved hjelp av GIS og geofysiske metoder. Master Thesis, Faculty of Social Sciences and Technology, Norges teknisk-naturvitenskapelige universitet, Trondhiem.

Larsen, B.P., S.J. Holdaway, P.C. Fanning, T. Mackrell and J.I. Shiner 2017 Shape as an outcome of formation history: Terrestrial laser scanning of shell mounds from far north Queensland, Australia. Quaternary International 427(A):5-12. https://doi.org/10.1016/j.quaint.2015.06.066

Lowe, K. 2010 Archaeological Site Testing along the Mississippi Gulf Coast: Cultural Resources Investigations on Hancock and Harrison Counties Mississippi. Baton Rouge, LA: Coastal Environments, Inc.

Moffat, I., L.A. Wallis, A. Beale and D. Kynuna 2008 Trialing geophysical techniques in the identification of open Indigenous sites in Australia: A case study from inland northwest Queensland. Australian Archaeology 66:60-63. http://dx.doi.org/10.1080/03122417.2008.11681868

Moss, P.T., S. Ulm, L. Mackenzie, L.A. Wallis, D. Rosendahl and L. Steinberger in press Robust local vegetation records from dense archaeological shell matrixes: A palynological analysis of the Thundiy shell deposit, Bentinck Island, Gulf of Carpentaria, Australia. Archaeological and Anthropological Sciences. https://doi-org.elibrary.jcu.edu.au/10.1007/s12520-016-0394-0

Nagel, T., D. Rosendahl, Q. Hua, P. Moss, C. Sloss, F. Petchey and S. Ulm 2016 Extended residence times for foraminifera in a marine-influenced terrestrial archaeological deposit and implications for palaeoenvironmental reconstruction. Journal of Archaeological Science: Reports 5:25-34. https://doi.org/10.1016/j.jasrep.2015.11.008

Navarro, F.J., A. Martín-Español, J.J. Lapazaran, M. Grabiec, J. Otero, E.V. Vasilenko and D. Puczko 2014 Ice volume estimates from ground-penetrating radar surveys, Wedel Jarlsberg Land Glaciers, Svalbard. Arctic, Antarctic, and Alpine Research 46(2):394-406. http://dx.doi.org/10.1657/1938-4246-46.2.394

Neal, A., J. Richards and K. Pye 2002 Structure and development of shell cheniers in Essex, southeast England, investigated using high-frequency ground-penetrating radar. Marine Geology 185(3):435-469. https://doi.org/10.1016/S0025-3227(01)00239-0

Nowroozi, A.A., G.R. Whittecar and J.C. Daniel 1997 Estimating the yield of crushable stone in an alluvial fan deposit by electrical resistivity methods near Stuarts Draft, Virginia. Journal of Applied Geophysics 38(1):25-40. https://doi.org/10.1016/S0926-9851(97)00014-1

O'Neil, D.H. 1993 Excavation sample size: A cautionary tale. American Antiquity 58(3):523-529. https://doi.org/10.2307/282111

Peck, H. 2016 The Application of Ecological Models and Trophic Analyses to Archaeological Marine Fauna Assemblages: Towards Improved Understandings of Prehistoric Marine Fisheries and Ecosystems in Tropical Australia. Unpublished PhD thesis, College of Arts and Society and Education, James Cook University, Cairns.

Pluckhahn, T.J., V.D. Thompson, N. Laracuente, S. Mitchell, A. Roberts and A. Sams 2009 Archaeological Investigations at the Famous Crystal River Site (8cI1) (2008 Field Season), Citrus County, Florida. Tampa: The University of South Florida.

Pluckhahn, T.J., V.D. Thompson and W.J. Rink 2016 Evidence for stepped pyramids of shell in the Woodland Period of eastern North America. American Antiquity 81(2):345-363. https://doi.org/10.7183/0002-7316.81.2.345

Pluckhahn, T.J., V.D. Thompson and B.R. Weisman 2010 Toward a new view of history and process at Crystal River (8CI1). Southeastern Archaeology 29(1):164-181. http://dx.doi.org/10.1179/sea.2010.29.1.011

Poteate, A.S. and S.M. Fitzpatrick 2013 Testing the efficacy and reliability of common zooarchaeological sampling strategies: A case study from the Caribbean. Journal of Archaeological Science 40(10):3693-3705. https://doi.org/10.1016/j.jas.2013.04.014

Prinz, R., A. Fischer, L. Nicholson and G. Kaser 2011 Seventy-six years of mean mass balance rates derived from recent and re-evaluated ice volume measurements on tropical Lewis Glacier, Mount Kenya. Geophysical Research Letters 38(20):L20502. https://doi.org/10.1029/2011GL049208

Rodrigues, S.I., J.L. Porsani, P.C.F. Giannini, M. Fornari, T. Atorre, P. DeBlasis and D.M.G. Ruiz 2015 Radarfacies and sedimentological analysis: Study of sedimentary substrate from an archaeological site (shell mound), southern Brazil. The Holocene 25(8):1257-1270. https://doi.org/10.1177/0959683615581202

Rodrigues, S.I., J.L. Porsani, V.R.N. Santos, P.A.D. DeBlasis and P.C.F. Giannini 2009 GPR and inductive electromagnetic surveys applied in three coastal sambaqui (shell mounds) archaeological sites in Santa Catarina state, South Brazil. Journal of Archaeological Science 36(10):2081-2088. https://doi.org/10.1016/j.jas.2009.05.013

Rosendahl, D., K.M. Lowe, L.A. Wallis and S. Ulm 2014 Integrating geoarchaeology and magnetic susceptibility at three shell mounds: A pilot study from Mornington Island, Gulf of Carpentaria, Australia. Journal of Archaeological Science 49:21-32. https://doi.org/10.1016/j.jas.2014.04.017

Rucker, D.F., G.E. Noonan and W.J. Greenwood 2011 Electrical resistivity in support of geological mapping along the Panama Canal. Engineering Geology 117(1-2):121-133. https://doi.org/10.1016/j.enggeo.2010.10.012

Sambuelli, L. and S. Bava 2012 Case study: A GPR survey on a morainic lake in northern Italy for bathymetry, water volume and sediment characterization. Journal of Applied Geophysics 81:48-56. https://doi.org/10.1016/j.jappgeo.2011.09.016

Santos, V.R.N., J.L. Porsani, C.A. Mendonça, S.I. Rodrigues and P.D. DeBlasis 2009 Reduction of topography effect in inductive electromagnetic profiles: Application on coastal sambaqui (shell mound) archaeological site in Santa Catarina state, Brazil. Journal of Archaeological Science 36(10):2089-2095. https://doi.org/10.1016/j.jas.2009.05.014

Shenkel, J.R. 1986 An additional comment on volume calculations and a comparison of formulae using several southeastern mounds. Midcontinental Journal of Archaeology 11(2):201-220.

Sorant, P.E. and J.R. Shenkel 1984 The calculation of volumes of middens, mounds, and strata having irregular shapes. American Antiquity 49(3):599-603. https://doi.org/10.2307/280363

Tetegan, M., C. Pasquier, A. Besson, B. Nicoullaud, A. Bouthier, H. Bourennane, C. Desbourdes, D. King and I. Cousin 2012 Field-scale estimation of the volume percentage of rock fragments in stony soils by electrical resistivity. Catena 92:67-74. https://doi.org/10.1016/j.catena.2011.09.005

Thompson, V.D. 2007 Articulating activity areas and formation processes at the Sapelo Island shell ring complex. Southeastern Archaeology 26(1):91-107.

Thompson, V.D. and C.F.T. Andrus 2011 Evaluating mobility, monumentality, and feasting at the Sapelo Island shell ring complex. American Antiquity 76(2):315-343. https://doi.org/10.7183/0002-7316.76.2.315

Thompson, V.D. and T.J. Pluckhahn 2010 History, complex hunter-gatherers, and the mounds and monuments of Crystal River, Florida, USA: A geophysical perspective. Journal of Island and Coastal Archaeology 5(1):33-51. http://dx.doi.org/10.1080/15564890903249811

Thompson, V.D., M.D. Reynolds, B. Haley, R. Jefferies, J.K. Johnson and L. Humphries 2004 The Sapelo shell ring complex: Shallow geophysics on a Georgia sea island. Southeastern Archaeology 23(2):192-201.

Treganza, A.E. and S.F. Cook 1948 The quantitative investigation of aboriginal sites: Complete excavation with physical and archaeological analysis of a single mound. American Antiquity 13(4):287-297. https://doi.org/10.2307/275295

Van Heteren, S., D.M. FitzGerald, D.C. Barber, J.T. Kelley and D.F. Belknap 1996 Volumetric analysis of a New England barrier system using ground-penetrating-radar and coring techniques. The Journal of Geology 104(4):471-483.

Wang, P., Z. Li, W. Wang, H. Li and F. Wang 2014 Glacier volume calculation from ice-thickness data for mountain glaciers – A case study of glacier No. 4 of Sigong River over Mt. Bogda, eastern Tianshan, Central Asia. Journal of Earth Science 25(2):371-378. https://doi.org/10.1007/s12583-014-0427-5

Weill, P., B. Tessier, D. Mouazé, C. Bonnot-Courtois and C. Norgeot 2012 Shelly cheniers on a modern macrotidal flat (Mont-Saint-Michel bay, France) – Internal architecture revealed by ground-penetrating radar. Sedimentary Geology 279:173-186. https://doi.org/10.1016/j.sedgeo.2010.12.002

Yde, J.C., M.K. Gillespie, R. Loland, H. Ruud, S.H. Mernild, S. De Villiers, N.T. Knudsen and J.K. Malmros 2014 Volume measurements of Mittivakkat Gletscher, southeast Greenland. Journal of Glaciology 60(224):1199-1207. https://doi.org/10.3189/2014JoG14J047
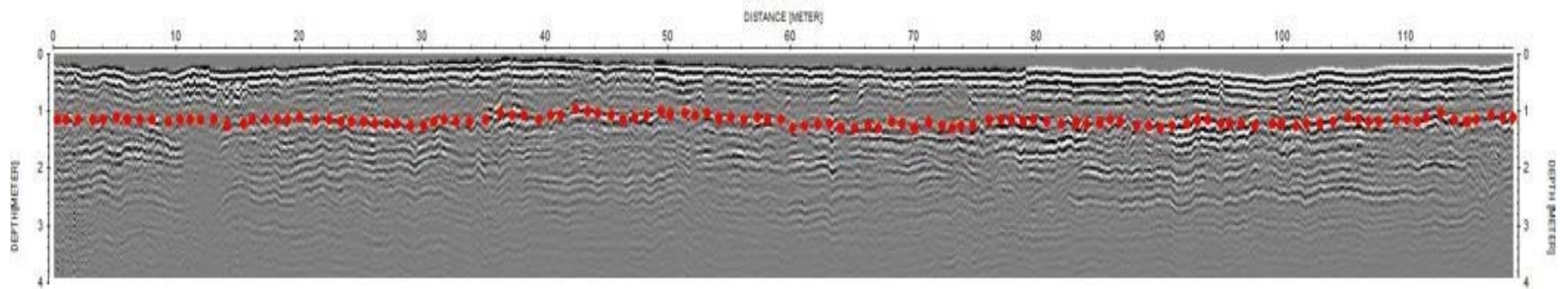
Supplementary Data

Thundiy GPR Line 3 of Transect A-B; this line was located in Transect A.
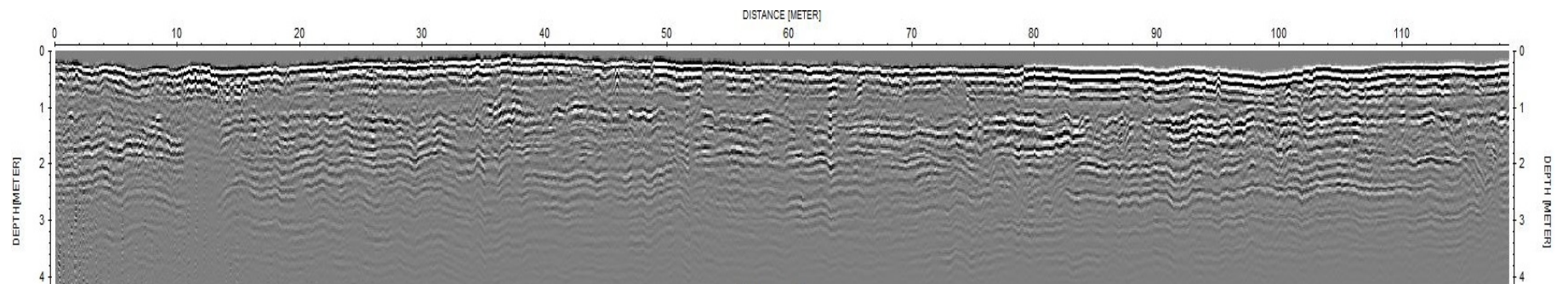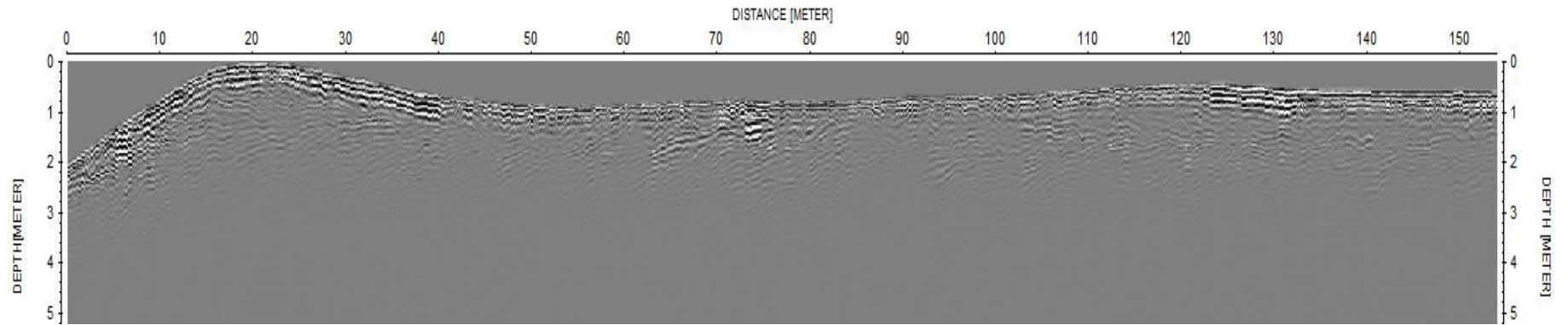
Line 3 showing the 'picks' marking the lower boundary of the cultural shell deposit.
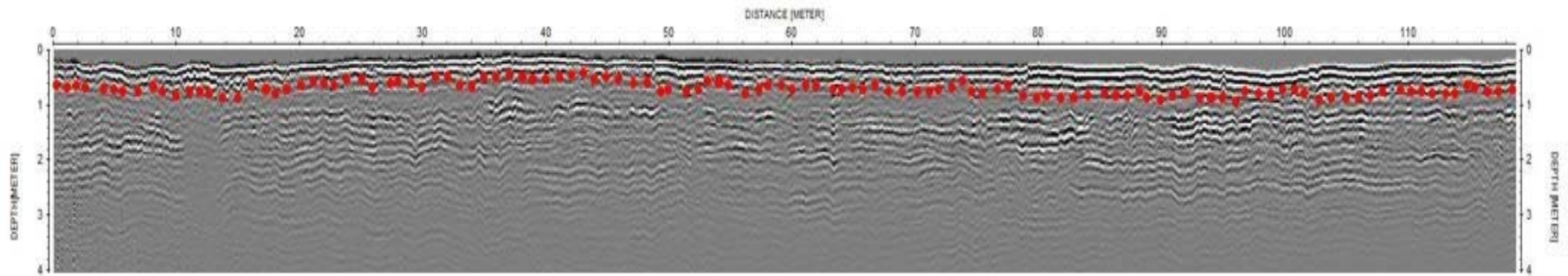
Line 3 showing the 'picks' marking the upper boundary of the beachrock deposit; where tree roots obscured the deposit from 10-12m the location of the deposit boundary was estimated.

26

Thundiy GPR Line 5 of Transect C.

Line 5 showing the 'picks' marking the shell matrix deposit above the beachrock.